

# Static and Dynamic of the Azide Anion Confined in an Armchair Carbon Nanotube

Stefano Battaglia

July 26, 2017

## 1 Computational Details

### 1.1 Ab-initio

In this work, the (5,5) armchair carbon nanotubes have been treated as finite-size systems, with the addition of hydrogen atoms at both ends in order to complete the valence shell. The nanotubes geometries have been optimized at DFT level of theory, employing the B97D3 exchange-correlation functional[1] in conjunction with the correlation consistent cc-pvtz gaussian basis set[2]. All the optimized structures retained their high symmetry, formally belonging to the  $D_{5d}$  molecular point group. Since nanotubes of different lengths have been considered throughout the work, we introduce the notation  $\Lambda$ -CNT(5,5) to label a nanotube composed by  $\Lambda$  [10]cyclophenacene units (cf. [cite]). The C–C bonds parallel ( $C-C_{\parallel}$ ) and perpendicular ( $C-C_{\perp}$ ) to the principal axis show the alternation pattern typical of these systems when treated as finite clusters[3, 4].

The geometry of the  $N_3^-$  azide anion has been optimized at DFT level of theory too, with the same functional, but in conjunction with the augmented version of the Dunning basis set, the aug-cc-pvtz in order to better describe the more diffuse electron density. The N–N bond length measures 1.1874 Å and is in excellent agreement with the experimental value obtained in gas phase of 1.1884 Å[5]. The geometry optimizations of the fragments alone have been performed with the Gaussian 09 software package, revision d01[6], using the default convergence thresholds and the ultrafine grid for the functional integral calculation.

#### 1.1.1 Azide anion inside CNT

It has been recently shown[?] that the interaction between the two fragments does not change significantly their structure and that the completely relaxed complex structure is found to be with the azide anion sitting in the center of the nanotube, aligned to the principal axis. Therefore, the optimal adsorption distance between the azide anion and the inner wall of the carbon nanotube has been obtained by relaxing all internal coordinates connecting the two fragments, while keeping frozen those strictly belonging to the monomers only. To ensure that the relaxation process did not remain trapped in a local minimum and without knowing a priori the optimal adsorption distance of the  $N_3^-$  molecule, the optimization procedure has been started from four different geometries. In all cases, the anion has been placed parallel to the principal axis of the nanotube. Three starting geometries were chosen according to possible “adsorption” sites in which the central nitrogen atom of the azide was placed either over C–C bonds (*bond* (b) and *zigzag* (z) geometries) or in the center of an hexagonal ring of the CNT wall (*hollow* (h) geometry). The three starting sites are shown in Figure 1, along with their labels that will be used in

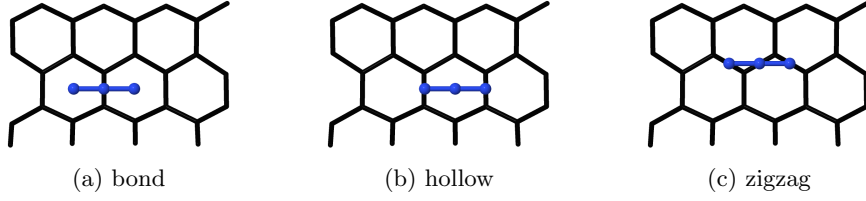


Figure 1: Starting sites of the bond, hollow and zigzag geometries, respectively.

the following to refer to them. For all three cases, the azide anion has been placed at a distance of about  $2.25\text{\AA}$  from the nanotube wall, well below the optima adsorption distance. The fourth starting geometry is shown in Figure 2 and it simply consists in the  $\text{N}_3^-$  anion placed exactly in

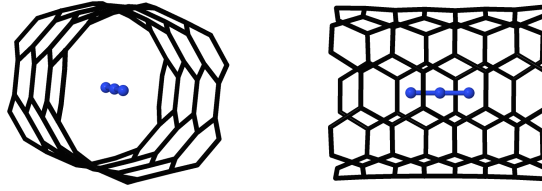


Figure 2: Central starting geometry (c). Note that the nanotube model has dangling hydrogen atoms at the two ends which are not shown here.

the center of the nanotube. We will refer to this starting geometry as *central* (c) geometry. In order to study the edge effects of the finite nanotube model, CNTs of four different lengths have been considered. The relaxation has been performed at density functional theory level using the B97D3 functional with the cc-pvdz basis set on the carbon nanotube and the aug-cc-pvtz on the  $\text{N}_3^-$ . The resolution-of-the-identity (RI) approximation has been used to compute the Coulomb part, adopting the universal fitting basis set def2/j[?]. The calculations have been performed using the ORCA 4 program package[?].

The relaxed structures starting from the (c) geometry correspond to a (local) minimum, as after one optimization step the convergence is reached, with the  $\text{N}_3^-$  anion insignificantly ( $\approx 0.002\text{\AA}$ ) shifted out of the principal axis. For this reason we will consider from now on the (c) geometry as the perfectly aligned anion to the principal axis and sitting in the center of the nanotube. For the three other starting conformations, namely the the (b), (h) and (z) geometries, the relaxation leads to different (local) minima. In order to analyze the differences in the final structures, three geometrical parameters and an energetic one have been considered. The geometrical parameters are depicted in Figure 3 and consist in the axial distance  $d_{cm}$  between the center of mass of the

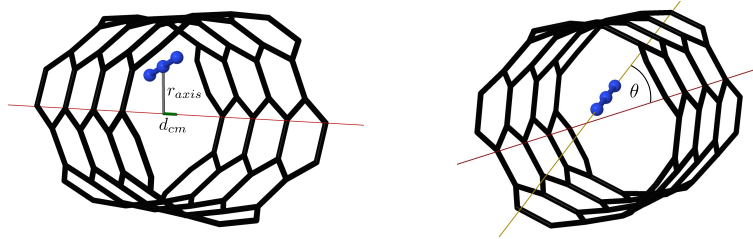


Figure 3: Geometrical parameters.

azide anion and the center of mass of the carbon nanotube, the radial distance  $r_{axis}$  of the azide anion center of mass from the principal axis of the nanotube and the angle  $\theta$  formed between the principal axis and an imaginary line passing through the external nitrogen atoms of the azide anion. The energetic parameter is the interaction energy  $E_{int}$  between the two fragments, computed as

$$E_{int} = E_{complex} - (E_{cnt} + E_{azide}) \quad (1)$$

and corrected for the basis set superposition error according to the Boys and Bernardi scheme[7]. Note that although geometry optimizations have been carried out on the complex systems, the geometry of the two fragments was kept frozen at the optimal fragment conformation, thus the value obtained from Equation (1) is only the interaction energy and not the binding energy of the system (i.e. it does not account for deformation effects).

The four parameters computed for all systems are listed in Table 1. Since the (c) geometry

$\Lambda$	site	$d_{cm}$ (Å)	$r_{axis}$ (Å)	$\theta$ (°)	$\Delta E_{int}$ (kcal/mol)
3	<i>bond</i>	0.018	0.002	0.06	-0.001
	<i>hollow</i>	0.002	0.003	0.04	0.000
	<i>zigzag</i>	0.000	0.003	0.27	-0.002
5	<i>bond</i>	0.604	0.009	0.32	0.112
	<i>hollow</i>	-0.144	0.002	0.32	0.017
	<i>zigzag</i>	0.000	0.003	0.43	0.000
7	<i>bond</i>	0.470	0.029	1.10	0.588
	<i>hollow</i>	-0.233	0.027	0.54	0.417
	<i>zigzag</i>	0.001	0.038	0.18	0.363
9	<i>bond</i>	0.622	0.015	0.74	0.400
	<i>hollow</i>	-1.304	0.003	0.17	0.030
	<i>zigzag</i>	-0.007	0.004	0.53	0.141

Table 1: Geometrical parameters and interaction energy difference with respect to the (c) geometry. Note that the  $d_{cm}$ ,  $r_{axis}$  and  $\theta$  are all zero for the (c) geometry.

consists in the azide ion sitting in the exact center of the nanotube, the three conformational parameters are all zero in this case, thus for geometries (b), (h) and (z), the parameters can be considered as differences from the (c) geometry. Accordingly, instead of tabulating the interaction energy for every geometry, the values listed in the last column of Table 1 correspond to the interaction energy difference between the (c) geometry and the other three, i.e.  $\Delta E_{int} = E_{int}(c) - E_{int}(site)$ . A negative value for  $\Delta E_{int}$  means that the interaction energy is more favorable (i.e. stronger) for the (c) geometry, while a positive value the opposite.

For all final geometries, the azide anion is found to be almost perfectly aligned to the principal axis of the nanotube since the angle  $\theta$  is always very small (below 1° except in one case), confirming the results presented in [?]. Similarly,  $r_{axis}$  is also always particularly small (most of the times below 0.01 Å), meaning that the anion has the preference to stay approximately at the same distance from the nanotube wall in all directions. In particular, independently from the length  $\Lambda$ , the azide ion is adsorbed at a distance of approximately 3.34 Å (computed as the distance between the  $N_3^-$  center of mass and the closest side of the wall). This value is significantly larger than the adsorption distance of 3.17 Å found for the confinement in a larger 3-CNT(6,6), obtained following the same computational procedure. There are two possible explanations for the difference in the adsorption distance. Either the different curvature of the two nanotubes is

such that the forces attracting the ion are stronger in the case of the (6,6) CNT, or in the case of the (5,5) CNT, there is a competition between the attractive forces exerted by the surrounding wall on the azide ion, which eventually stabilizes it at an (almost) equal radial distance in any direction. The analysis of the curvature effects on the adsorption distance inside the CNT are beyond the scope of this work, and thus not further investigated here [maybe there are refs for other systems, probably H<sub>2</sub> and H<sub>2</sub>O]. The most fluctuating parameter is  $d_{cm}$ . Clearly, the periodic atomic pattern of the carbon nanotube makes the potential energy surface (PES) of the complex full of local minima, all of which approximately share the same well depth. Apart from the (z) conformation, for which  $d_{cm}$  remains virtually unchanged irrespective of the length, it is hard to rationalize the results for the (b) and (h) cases. The only exception is found for the 3-CNT(5,5), where the two open ends of the nanotube are so close that the energy barriers to move away from the center are particularly steep. Nonetheless, although the evident difference between the final geometries, the effect observed on the interaction energy, which is our first and most important parameter that we are interested in, is minimal and, importantly, below chemical accuracy ( $\approx 1$  kcal/mol). As it appears a very hard task to find the *global minimum* for this type of systems and considering the small influence observed on the interaction energy as well as remembering that the accuracy of classical parametrized potentials is well below the differences  $\Delta E_{int}$  listed in Table 1 [maybe ref?], the central geometry (c) will be used for all interaction energies computed in this work at a higher level of theory or for nanotubes longer than  $\Lambda = 9$ . An extensive test on the dependence of the length of the nanotube and the basis set size with respect to the interaction energy has been performed. In Figure 4 we see the resulting values.

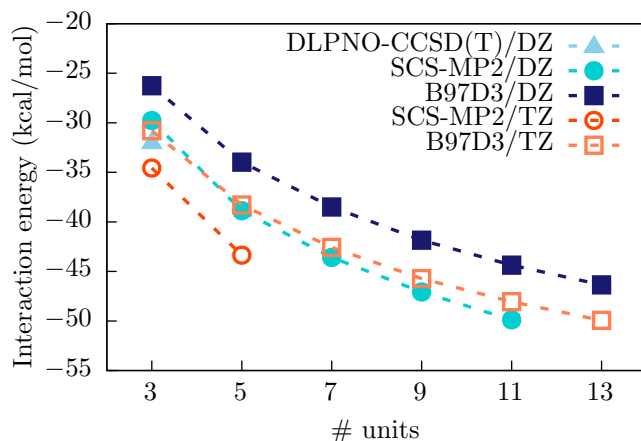


Figure 4: Interaction energy dependence on the nanotube length.

## 1.2 Molecular Dynamics

The Improved Lennard-Jones (ILJ) potential is given by

$$V_{ILJ}(r) = \epsilon \left[ \frac{m}{n(r) - m} \cdot \left( \frac{r_0}{r} \right)^{n(r)} - \frac{n(r)}{n(r) - m} \cdot \left( \frac{r_0}{r} \right)^m \right] \quad (2)$$

where

$$n(r) = \beta + 4.0 \cdot \left( \frac{r}{r_0} \right)^2 \quad (3)$$

and  $r = R_{i,j}$  is the distance between carbon atom  $i$  and nitrogen atom  $j$ . The parameters  $r_0$ ,  $\epsilon$  and  $\beta$  are set according to the atoms interacting, while  $m$  is set according to the partial charges of the interacting species. The induction potential term for a  $\text{N}_3^-$  anion interacting with carbon atoms is given by

$$V_{ind}(R_{i,1}, R_{i,2}, R_{i,3}) = -\frac{1}{2} \cdot \alpha_C \cdot \frac{n(R_{i,2})}{n(R_{i,2}) - 4} \left[ \frac{Q_{N_1}}{R_{i,1}^2} + \frac{Q_{N_2}}{R_{i,2}^2} + \frac{Q_{N_3}}{R_{i,3}^2} \right]^2 \quad (4)$$

where  $R_{i,1}$ ,  $R_{i,2}$  and  $R_{i,3}$  are the distances between the carbon atom  $i$  and the three nitrogen atoms,  $Q_{N_1}$ ,  $Q_{N_2}$  and  $Q_{N_3}$  are the partial charges on the nitrogen atoms,  $\alpha_C$  is the polarizability of the carbon atoms and  $n(R_{i,2})$  is equal to  $n(r)$  using  $r_0$  according to the interaction between  $\text{C} - \text{N}_2$ .

Because we are using a finite-size model for the carbon nanotube, saturated with hydrogen atoms at the two ends, the nanotube wall is polarized. The interaction between the azide anion and the nanotube contains therefore a significant electrostatic contribution, which cannot be neglected. The electrostatic potential term is given by the following formula

$$V_{els}(R_{i,j}) = \sum_{i,j} \frac{Q_i Q_j}{R_{i,j}} \quad (5)$$

where the sum runs over all atoms of the two fragments and takes into account all pairwise electrostatic interactions between them. The total interaction energy between the azide anion confined inside a carbon nanotube is given by

$$E_{int} = \left[ \sum_{i=1}^{N_C} V_{ind}(R_{i,1}, R_{i,2}, R_{i,3}) + \sum_{j=1}^{N_N} V_{ILJ}^{C-N_j}(R_{i,j}) + V_{els}(R_{i,j}) \right] + \sum_{k=1}^{N_H} \sum_{j=1}^{N_N} V_{els}(R_{k,j}) \quad (6)$$

where  $N_C$ ,  $N_N$  and  $N_H$  correspond to the total number of carbon, nitrogen and hydrogen atoms, respectively. The ILJ potential  $V_{ILJ}^{C-N_j}$  is defined according to the parameters given in Table 2 and

atom types	$\epsilon$	$r_0$	$\beta$	$m$
C-N <sub>1,3</sub>	5.205	3.994	6-9	6.0
C-N <sub>2</sub>	3.536	3.828	6-9	6.0

Table 2: ILJ parameters for the interaction of  $\text{N}_3^-$  confined inside a carbon nanotube. Different values of  $\beta$  are tested.

the polarizability  $\alpha_C$  appearing in  $V_{ind}$  is set to 1.2, the partial charges as  $Q_{N_1} = Q_{N_3} = -0.56$  and  $Q_{N_2} = 0.12$  and finally the term  $\frac{n}{n-4}$  is assumed to be 1.0 for the time being.

In order to test the performance of the classical potential, we have computed the interaction energy between the azide anion and a short 3-CNT(5,5) nanotube at *ab-initio* level and compared it with the result obtained by the potential, as shown in Table 3.

Similarly, we have compared the interaction energies for the confinement in a longer 5-CNT(5,5), listed in Table 4. Moreover, Table 5, Table 6 and Table 7 list the results for longer nanotubes. A comparison of the interaction energy computed by different dft functionals is listed in Table 8, while a comparison of the electrostatic term with respect to the basis set used in the calculation can be seen in Table 9.

Terms	$\beta = 7.0$	$\beta = 8.0$	$\beta = 9.0$
$V_{ILJ}$ [kcal/mol]	-10.90	-9.68	-8.37
$V_{els}$ [kcal/mol]	+42.24	+42.24	+42.24
$V_{ind}$ [kcal/mol]	-52.91	-52.91	-52.91
$V_{tot}$ [kcal/mol]	-21.57	-20.35	-19.04
$V_{CCSD(T)}$ [kcal/mol]		-31.96	
$V_{MP2/DZ}$ [kcal/mol]		-29.77	
$V_{MP2/TZ}$ [kcal/mol]		-34.56	

Table 3: Interaction energies for  $N_3^-$  confined inside a 3-CNT(5,5).

Terms	$\beta = 7.0$	$\beta = 8.0$	$\beta = 9.0$
$V_{ILJ}$ [kcal/mol]	-12.33	-11.15	-9.89
$V_{els}$ [kcal/mol]	+27.55	+27.55	+27.55
$V_{ind}$ [kcal/mol]	-56.83	-56.83	-56.83
$V_{tot}$ [kcal/mol]	-41.61	-40.43	-39.16
$V_{MP2/DZ}$ [kcal/mol]		-38.87	
$V_{MP2/TZ}$ [kcal/mol]		-43.36	

Table 4: Interaction energies for  $N_3^-$  confined inside a 5-CNT(5,5).

Terms	$\beta = 7.0$	$\beta = 8.0$	$\beta = 9.0$
$V_{ILJ}$ [kcal/mol]	-12.79	-11.66	-10.46
$V_{els}$ [kcal/mol]	+18.70	+18.70	+18.70
$V_{ind}$ [kcal/mol]	-57.71	-57.71	-57.71
$V_{tot}$ [kcal/mol]	-51.81	-50.68	-49.48
$V_{MP2/DZ}$ [kcal/mol]		-43.58	

Table 5: Interaction energies for  $N_3^-$  confined inside a 7-CNT(5,5).

Terms	$\beta = 7.0$	$\beta = 8.0$	$\beta = 9.0$
$V_{ILJ}$ [kcal/mol]	-12.73	-11.58	-10.37
$V_{els}$ [kcal/mol]	+13.64	+13.64	+13.64
$V_{ind}$ [kcal/mol]	-58.27	-58.27	-58.27
$V_{tot}$ [kcal/mol]	-57.36	-56.22	-55.00
$V_{MP2/DZ}$ [kcal/mol]		-47.07	

Table 6: Interaction energies for  $N_3^-$  confined inside a 9-CNT(5,5).

Terms	$\beta = 7.0$	$\beta = 8.0$	$\beta = 9.0$
$V_{ILJ}$ [kcal/mol]	-12.67	-11.52	-10.28
$V_{els}$ [kcal/mol]	+10.60	+10.60	+10.60
$V_{ind}$ [kcal/mol]	-58.54	-58.54	-58.54
$V_{tot}$ [kcal/mol]	-60.61	-59.46	-58.23
$V_{MP2/DZ}$ [kcal/mol]	-49.88		

Table 7: Interaction energies for  $N_3^-$  confined inside a 11-CNT(5,5).

SCS-MP2	B97-D3	BLYP-D3	rPW86PBE-D3	wB97X-D3	TPSS0-D3	B3LYP-D3	PW6B95-D3
-2.19	-5.70	-4.99	-6.89	-6.28	-8.08	-6.88	

Table 8: Interaction energy differences of various density functionals with respect to the reference DLPNO-CCSD(T) value for  $N_3^-$  confined inside a 3-CNT(5,5).

$\Lambda$	cc-pvdz	cc-pvtz	cc-pvqz
3	48.20	42.24	45.20
5	31.46	27.55	28.78

Table 9: Comparison of electrostatic contribution in kcal/mol with respect to the basis set used in the calculation to obtain the partial atomic charges.

Since the aim is to fit the potential to the max interaction energy only (i.e. to fit the well depth  $\epsilon$ ), a very accurate value for this interaction energy is required. In order to do so, an elaborate scheme is required, which involves several steps.

1. Geometry relaxation of the complex system and the monomers. The nanotube length is only 3 units, otherwise there are too many basis functions
  - (a) Using one pure functional among PBE, B97 and TPSS
  - (b) Using Grimme dispersion with Becke and Johnson damping (D3BJ)
  - (c) Using the cc-pvtz basis set on the CNT and the aug-cc-pvtz on the nitrogen (diffuse functions also on the tube lead to linear dependence)
  - (d) Now testing density fitting in Gaussian, if much faster, we use also that for the pure functional with the universal def2/j basis set
  - (e) Using one hybrid functional among B3LYP, APFD, what else?
2. All the geometry calculations are performed in Gaussian
3. To obtain accurate interaction energies, there is a total of 7 single point calculations to be performed
  - (a) Complex at the complex geometry in the full basis
  - (b) First monomer at the complex geometry in the full basis
  - (c) First monomer at the complex geometry in the monomer basis
  - (d) First monomer at the monomer geometry in the monomer basis
  - (e) Second monomer at the complex geometry in the full basis
  - (f) Second monomer at the complex geometry in the monomer basis
  - (g) Second monomer at the monomer geometry in the monomer basis
4. The series of 7 calculations just listed has to be done for two basis sets, to be able to extrapolate the results at CBS limit
5. The extrapolation schemes are different for SCF and correlated calculations, therefore they can be done separately
6. For the SCF extrapolation, we can compute in Gaussian using triple and quadruple zeta basis sets
7. For the correlated extrapolation, we can compute in ORCA using double and triple zeta basis sets (which will give us also dz scf points)
8. The SCF in this case does not use the RI approximation for both Gaussian and ORCA
9. The correlated method is the DLPNO-CCSD(T)
10. Partial charges have to be obtained and there are many ways to do it. First of all, we need to decide which density to use
  - (a) The density (relaxed, unrelaxed, linearized?) of the DLPNO-CCSD(T) method (I do not know how much expensive it is)



- (b) Find a DFT functional in which we can trust (how?) and use its density
  - (c) Use the density of DLPNO-SCS-MP2 if it reproduces well the CCSD(T) one. But the same problem as above (relaxed, unrelaxed, linearized? Expensive?)
11. Once we know which density we want to use, calculate the charges
    - (a) NPA charges from NBO analysis
    - (b) MESP derived charges
    - (c) Many other possibilities...
  12. Calculate multipole moments with the charges obtained and compare them with the moments obtained from the calculation

The above computational scheme will provide a very accurate interaction energy and can be ideally applied to different systems. The major pitfall of the above procedure, is the very first step, i.e. the geometry optimization.

1. The functional used for the geometry optimization might give wrong conformations
2. One should optimize the geometry using a wf method, but if it is too expensive we cannot
3. Moreover there are a plethora of minima in the PES, several starting geometries have to be relaxed and compared with each other

With the interaction energy and the partial charges, we can tune the ILJ potential such that it reproduces the interaction energy obtained with the above scheme.

There is a large amount of arbitrariness in this procedure to obtain the ILJ potential. The partial charges calculated are in principle arbitrary and considering them explicitly enhances the complexity of the problem. In particular, the charges will certainly vary depending on the length of the nanotube. This means that if we would like to use longer CNTs in the MD simulation, then the tuned ILJ potential which includes explicitly the charges might not be valid anymore. I believe that therefore we cannot pursue this approach.

A possible solution would be to fit the ILJ potential to a series of calculations of the complex system at different conformations. In this way, the electrostatic effects would be implicitly taken care of in the fitting procedure. Nonetheless, for such a fit, the above procedure is certainly too expensive and one should come up with a reasonable approximation.

Another possibility is to neglect completely the electrostatic term in the potential and tune it just according to dispersion and induction forces. This is basically the same as the above solution, but without fitting the entire potential and only relying on the single interaction energy value.

A last idea is to assume that in the limit of a very long nanotube, the polarization far away from the nanotube ends is minimal and has to be taken care only locally around the azide anion. This would mean that the partial charges are assigned only locally around the azide anion and they would need to be approximated in some way. One such way is to compute them for a nanotube of increasing length and observe how they change. If the change is minimal, they can be safely assumed to remain so for any length, if this is not the case, then probably this idea is not feasible.

## References

- [1] Stefan Grimme, Jens Antony, Stephan Ehrlich, and Helge Krieg. A consistent and accurate ab initio parametrization of density functional dispersion correction (DFT-D) for the 94 elements H-Pu. *J. Chem. Phys.*, 132(15), 2010.

- [2] Thom H. Dunning Jr. Gaussian basis sets for use in correlated molecular calculations. I. The atoms boron through neon and hydrogen. *J. Chem. Phys.*, 90(2):1007–1023, 1989.
- [3] Zhiyong Zhou, Michael Steigerwald, Mark Hybertsen, Louis Brus, and Richard A. Friesner. Electronic Structure of Tubular Aromatic Molecules Derived from the Metallic (5,5) Armchair Single Wall Carbon Nanotube. *J. Am. Chem. Soc.*, 126(11):3597–3607, mar 2004.
- [4] Annia Galano. On the influence of diameter and length on the properties of armchair single-walled carbon nanotubes: A theoretical chemistry approach. *Chem. Phys.*, 327(1):159–170, 2006.
- [5] Mark Polak, Martin Gruebele, and Richard J. Saykally. Velocity Modulation Laser Spectroscopy of Negative Ions: The  $\nu_3$  Band of Azide ( $\text{N}_3^-$ ). *J. Am. Chem. Soc.*, 109(10):2884–2887, may 1987.
- [6] M. J. Frisch, G. W. Trucks, H. B. Schlegel, Gustavo E. Scuseria, M. A. Robb, J. R. Cheeseman, Giovanni Scalmani, Verónica Barone, Benedetta Mennucci, George A. Petersson, H. Nakatsuji, M. Caricato, X. Li, H. P. Hratchian, A. F. Izmaylov, J. Bloino, G. Zheng, J. L. Sonnenberg, M. Hada, M. Ehara, K. Toyota, R. Fukuda, J. Hasegawa, M. Ishida, T. Nakajima, Y. Honda, O. Kitao, H. Nakai, T. Vreven, J. A. Montgomery Jr., J. E. Peralta, F. Ogliaro, M. Bearpark, J. J. Heyd, E. Brothers, K. N. Kudin, V. N. Staroverov, R. Kobayashi, J. Normand, K. Raghavachari, A. Rendell, J. C. Burant, S. S. Iyengar, J. Tomasi, M. Cossi, N. Rega, J. M. Millam, M. Klene, J. E. Knox, J. B. Cross, V. Bakken, C. Adamo, J. Jaramillo, R. Gomperts, R. E. Stratmann, O. Yazyev, A. J. Austin, R. Cammi, C. Pomelli, J. W. Ochterski, R. L. Martin, K. Morokuma, V. G. Zakrzewski, G. A. Voth, P. Salvador, J. J. Dannenberg, S. Dapprich, A. D. Daniels, Ö. Farkas, J. B. Foresman, J. V. Ortiz, J. Cioslowski, and D. J. Fox. Gaussian 09 Revision D.01.
- [7] S. F. Boys and F. Bernardi. The calculation of small molecular interactions by the differences of separate total energies. Some procedures with reduced errors. *Mol. Phys.*, 19(4):553–566, 1970.